European Journal of Cancer 169 (2022) 64–73

Available online at www.sciencedirect.com

ScienceDirect

journal homepage: www.ejcancer.com

Original Research

High tumor mutational burden (TMB) identifies a microsatellite stable pancreatic cancer subset with prolonged survival and strong anti-tumor immunity

Eva Karamitopoulou [a,*], Andreas Andreou [b], Anna Silvia Wenning [b], Beat Gloor [b,1], Aurel Perren [a,1]

[a] *Institute of Pathology, University of Bern, Switzerland*
[b] *Department of Visceral Surgery, Insel University Hospital, University of Bern, Switzerland*

Received 13 January 2022; received in revised form 24 February 2022; accepted 23 March 2022

KEYWORDS
Tumor mutational burden;
Microsatellite instability;
Pancreatic cancer;
Immunotherapy;
Immune response

Abstract ***Aim:*** Tumor mutational burden (TMB: somatic mutations per megabase, mut/Mb) predicts the efficacy of immunotherapy. Here, we link TMB levels with the activation of immune pathways and intratumoral immune responses in pancreatic adenocarcinoma (PDAC) to explore immunoarchitectural patterns associated with high TMB.
Methods: We assessed TMB in 161 resected, microsatellite stable (MSS) PDACs, including 41 long-term survivors (LTS). Five microsatellite instable (MSI-high) cases were also assessed. Cases were classified into TMB-high (≥10 mut/Mb), TMB-intermediate (>5 < 10 mut/Mb), and TMB-low (≤5 mut/Mb) categories. Tumors additionally underwent mRNA *in situ* hybridization for immune pathway genes and were immunoprofiled by multiplex immunofluorescence followed by automated image analysis.
Results: We detected 12 TMB-high, 28 TMB-intermediate, and 121 TMB-low cases. TMB-high tumors comprised ten LTSs (10/41; 24%) and two conventional PDACs (2/120; 1.7%). They exhibited the highest T cell density with significantly increased $CD3^+CD4^+$T helper and $CD208^+$dendritic cell (DC) counts, compared to all other cases. $CD3^+CD8^+$cytotoxic T cells were significantly closer to tumor cells and T helper cells closer to DCs in TMB-high PDACs. Immune pathways involved in T cell activation, immune cell adhesion/migration, antigen presentation, and cytokine signaling were upregulated in most TMB-high and many TMB-intermediate tumors. *ARID1A* and *ERBB4* alterations were more frequent in TMB-high PDACs. All MSI-high PDACs were TMB-high.

* *Corresponding author*: Pancreatic Cancer Research, Institute of Pathology, University of Bern, Senior Consultant, Pancreatobiliary and GI-Pathology, Pathology Institute Enge, Hardturmstr. 133, 8005, Zurich, Switzerland.
E-mail address: eva.diamantis@patho.ch, eva.diamantis@pathology.unibe.ch (E. Karamitopoulou).
[1] Equally contributing authors.

https://doi.org/10.1016/j.ejca.2022.03.033

Conclusions: TMB-high cases frequently belong to specific PDAC subsets with prolonged survival such as LTSs and MSI-high PDACs. They display strong anti-tumor immune responses fueled by a T helper cell/DC-mediated priming of the cytotoxic T cells. Moreover, they frequently harbor further actionable alterations.

1. Introduction

Programmed death receptor-1/ligand 1 (PD-1/L1) antibodies can induce durable remissions and improve outcomes in many malignancies [1]. However, response rates are low in unselected patients, as compared with selected groups such as patients with microsatellite instability-high (MSI-high)/mismatch repair-deficient (dMMR) tumors where PD-1/PD-L1 blockade has been shown to be highly effective [2,3]. The sensitivity of MSI-high tumors to PD-1 blockade might be related to their high tumor mutational burden (TMB), which has been shown to predict checkpoint blockade response in many cancer types [4–6]. TMB is broadly defined as the number of somatic mutations per megabase of interrogated genomic sequence [7] and is believed to be a key driver in the generation of immunogenic neo-peptides displayed on major histocompatibility complexes (MHC) on the tumor cell surface [4,7]. Tumor-specific neo-antigens arise from somatic mutations [8,9] and play a pivotal role in tumor-specific T cell-mediated anti-tumor immunity after the inhibition of checkpoint signals [5,10]. Recently, US Food and Drug Administration (FDA) approved pembrolizumab monotherapy for solid tumor patients with TMB $\geq$10 mut/Mb [11].

So far, immunotherapy by using checkpoint inhibitors was not successful in pancreatic ductal adenocarcinoma (PDAC), mostly due to its immunosuppressive tumor microenvironment (TME) and the relatively low expression and/or low quality of tumor-specific neo-antigens except for a small subset of patients with high-quality neo-antigens due to the molecular mimicry of microbial epitopes [12,13]. Moreover, existing evidence about the correlation of TMB and neo-antigen expression with the effectiveness of checkpoint inhibition in microsatellite stable (MSS) PDACs is rather weak and needs further exploration [7,14]. The low immunogenicity of PDACs can be attributed to T cell dysfunction, despite the presence of tumor-infiltrating lymphocytes (TILs) in as many as 30% of patients, which points to failed T cell priming [15–18]. The immunosuppressive role of TME in PDAC is thought to be mediated by regulatory T cells (Tregs), tumor-associated macrophages (TAMs), myeloid-derived suppressor cells, and an increase in immunosuppressive cytokines [19].

Deeper knowledge of the factors, which might affect the response to checkpoint inhibitor therapy in PDAC would help to increase the number of patients who might benefit from this type of therapy. Here, we link different TMB levels with the immune response patterns within the TME as well as with the activation of immune pathways and the genetic changes of the tumor cells and reveal major immunologic differences among TMB subgroups, which might explain the different immunotherapy success rates.

2. Materials and Methods

2.1. Patient characteristics

From 349 consecutive PDAC patients, who underwent oncologic resection between 2003 and 2018 at the Department of Visceral Surgery and Medicine, Insel University Hospital, Bern, five cases (n = 5, 1.66%) were MSI-high. From the 344 MSS cases, 41 (11.9%) were long-term survivors (LTS, overall survival (OS) $\geq$ 60 months) [20,21]. From the remaining 303 PDACs, 289 MSS cases fulfilled the inclusion criteria such as full clinical and histopathologic information, enough available tumor tissue to perform the analyses, and conventional ductal adenocarcinoma histology. Cases with adenosquamous or mucinous histology as well as undifferentiated carcinomas were excluded. From these 289 cases, 120 randomly selected MSS PDACs were included into the study and comprised the cohort of the "conventional" MSS PDACs (cohort 1). The subgroup of 41 long-term survivors comprised the cohort 2 (LTS-cohort), whereas the five MSI cases were additionally analyzed for comparison (cohort 3: MSI-cohort). The study design is outlined in Suppl. Fig. S1. The clinicopathologic characteristics of all patient cohorts are summarized in Suppl. Table S1. The study was approved by the Ethics Commission of the Canton of Bern (KEK 2019–02212) and was carried out in accordance with the principles expressed in the Declaration of Helsinki. Detailed information about immunohistochemistry, tumor mutational load assay, mRNA in situ hybridization, multiplex immunofluorescence, image analysis, and statistical analysis can be found in Suppl. Material and Methods.

3. Results

3.1. Clinicopathological profiles and TMB

TMB values ranged in MSS-PDACs between 0.5 and 14.91 (median: 3.36, mean: 3.97). Cases were classified into TMB-high (≥10mut/Mb, n = 12), TMB-intermediate (>5 < 10mut/Mb, n = 28), and TMB-low (≤5mut/Mb, n = 121) categories. TMB-high cases included ten LTSs (10/41; 24%) and two conventional PDACs (2/120; 1.7%), and TMB-intermediate cases included nine LTSs (22%) and 19 conventional PDACs (15.8%), whereas TMB-low cases included 22 LTSs (54%) and 99 conventional PDACs (82.5%). Clinicopathological features of TMB categories are presented in Table 1. TMB-high cases displayed favorable features, such as higher proportion of grade 1 (p = 0.035) and lymph node negative cases (p = 0.034), lower proportion of venous invasion (p = 0.032), as well as prolonged OS (median 71 months; p = 0.001) and PFS (median 68 months; p = 0.001). In contrast, TMB-low tumors displayed higher grade (0.031) and nodal stage (p = 0.034) as well as worse overall (OS) and progression-free survival (PFS) (median OS: 13 months, median PFS: 7 months). TMB-intermediate tumors showed "in-between" features.

3.2. mRNA in situ hybridization

Unbiased hierarchical clustering of 70 PDACs (12 TMB-high, 28 TMB-intermediate, and 29 randomly selected TMB-low cases) led to the identification of three distinct clusters representing different activation levels of the 72 immune pathway genes (Fig. 1, Suppl. Table 2). The first cluster showed downregulation of all genes except *B2M*, which has been associated with immunotherapy resistance, *CD44*, which promotes cancer stemness, and *CTNNB1*, which is involved in Wnt signaling and promotes epithelial-mesenchymal

Table 1
Clinicopathological features of MSS PDACs across the three TMB categories.

	TMB ≥10 **(n = 12)**	TMB >5 < 10 **(n = 28)**	TMB ≤5 **(n = 121)**	P-value
TMB **median (range)**	12.23 (10.21–14.9)	6.70 (5.01–8.7)	2.51 (0.5–4.98)	
Sex				0.266
F	6 (50%)	17 (60.7%)	53 (43.8%)	
M	6 (50%)	11 (39.3%)	68 (56.2%)	
Age, median (range), years	74 (60–83)	69 (35–83)	65 (34–84)	**0.035**
Size, median (range), mm	30 (20–80)	30 (15–50)	30 (4–90)	0.536
Grade				**0.031**
G1	6 (50%)	6 (21.4%)	19 (15.7%)	
G2	1 (8.3%)	12 (42.9%)	57 (47.1%)	
G3	5 (41.7%)	10 (35.7%)	45 (37.2%)	
UICC Stage				0.098
IA	1 (8.3%)	1 (3.6%)	8 (6.6%)	
IB	4 (33.3%)	6 (21.4%)	13 (10.7%)	
IIA	2 (16.7%)	0 (0%)	5 (4.1%)	
IIB	3 (25%)	15 (53.6%)	63 (52.1%)	
III	2 (16.7%)	6 (21.4%)	32 (26.5%)	
T-stage				0.829
T1	1 (8.3%)	5 (17.9%)	21 (17.3%)	
T2	8 (66.7%)	19 (67.8%)	74 (61.2%)	
T3	3 (25%)	4 (14.3%)	26 (21.5%)	
N-stage				**0.034**
N0	7 (58.33%)	7 (25%)	23 (19%)	
N1	4 (33.33%)	17 (60.7%)	67 (55.4%)	
N2	1 (8.33%)	4 (14.3%)	31 (25.6%)	
L-Stage				0.101
L0	5 (41.7%)	5 (17.9%)	20 (16.5%)	
L1	7 (58.3%)	23 (23.1%)	101 (83.5%)	
V-Stage				**0.032**
V0	8 (66.7%)	10 (35.7%)	49 (40.5%)	
V1	4 (33.3%)	18 (64.3%)	72 (59.5%)	
Pn-Stage				**0.026**
Pn0	2 (16.7%)	1 (3.6%)	2 (1.6%)	
Pn1	10 (83.3%)	27 (94.4%)	119 (98.4%)	
R-Stage				0.255
R0	9 (75%)	16 (57.1%)	80 (66.1%)	
R1	3 (25%)	12 (42.9%)	41 (33.9%)	
OS, median (range), months	71 (5–197)	11 (0–169)	13 (1–200)	**0.001**
PFS, median (range), months	68 (3–192)	7 (0–162)	8 (0–196)	**0.001**

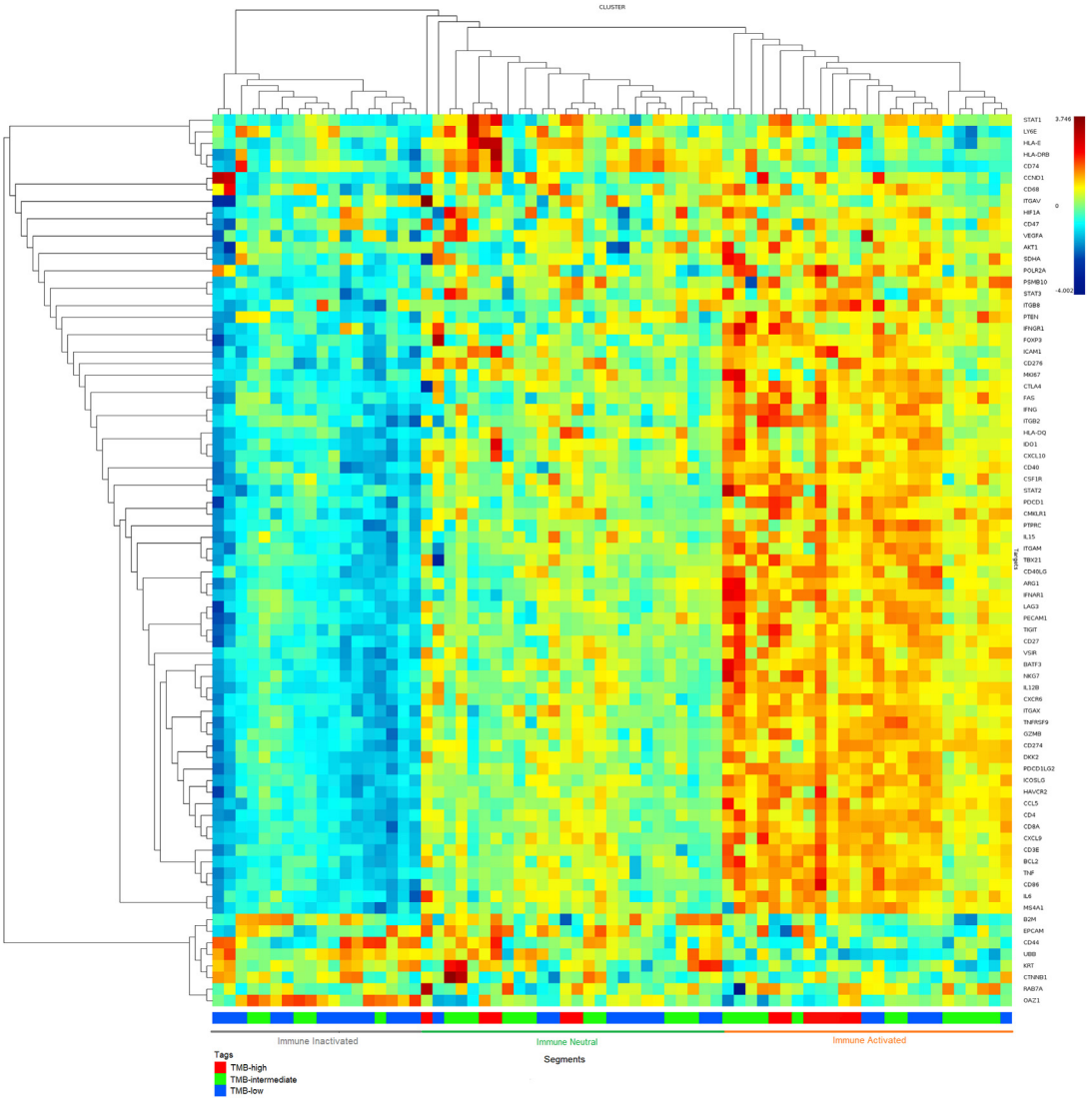

Fig. 1. Heatmap showing the differential expression of immune pathway-associated genes in PDACs of the three different TMB categories. Unbiased hierarchical clustering of the tumors led to the identification of three distinct clusters ("immune inactivated", "immune neutral", and "immune activated") representing different levels of activation of the 72 immune pathway-associated genes.

transition (EMT) [22–24]. This cluster was named "immune inactivated" and was enriched with TMB-low tumors (13/29; 44.8%), whereas five TMB-intermediate PDACs (5/28; 17.8%) clustered together. No TMB-high PDACs were found in this cluster. In contrast, the third cluster was characterized by two- to three-fold upregulation of almost all genes except *B2M*, *CD44,* and *CTNNB1*, which were downregulated. We named this cluster "immune activated" and included seven TMB-high (7/12; 58%), 12 TMB-intermediate (12/28; 42.8%), and six TMB-low PDACs (6/29; 20.7%; Fig. 1, Suppl. Fig. 2). The intermediate cluster, showing zero- to two-fold upregulation of most genes was named "immune neutral" and comprised five TMB-high (42%), 11 TMB-intermediate (39.3%), and ten TMB-low PDACs (34.5%; Fig. 1, Suppl. Fig. 2). In summary, most TMB-high PDACs clustered into the "immune activated" and the remaining into the "immune neutral" cluster, whereas TMB-low tumors mostly clustered into the "immune inactivated" and "immune neutral" clusters. TMB-intermediate PDACs clustered mostly into the "immune neutral" and "immune activated" clusters.

3.3. Immune response patterns and TMB

TMB-high tumors exhibited T cell-rich TMEs, characterized by numerous $CD3^+$, $CD3^+CD4^+$(FOXP3$^-$)T cells (T helper cells) and $CD3^+CD8^+$(PD-L1$^-$)T cells (cytotoxic T cells) as well as $CD208^+$dendritic cells (DCs) in both intraepithelial and stromal compartments (Figs. 2–4). DCs and T helper cells were particularly prominent, especially in the stromal compartment. In contrast, TMB-low cases were poor in cytotoxic as well as T helper cells and rich in $CD68^+$TAMs and regulatory

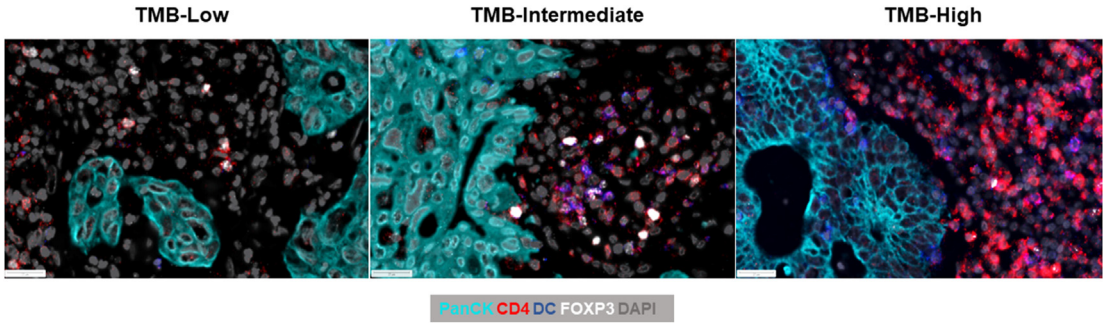

Fig. 2. Representative images of the immune microenvironment from tumors of the three TMB categories, depicting $CD3^+CD4+$ T cells (CD4, red), $CD208^+$ dendritic cells (DC, blue), and $CD3^+CD4^+FOXP3+$ T regulatory cells (FOXP3, white). The Pancytokeratin$^+$ tumor cells (PanCK) are depicted in cyanide and DAPI nuclear staining in grey. Multiple immune Fluorescence (mIF) x400. (For interpretation of the references to color in this figure legend, the reader is referred to the Web version of this article.)

$CD3^+CD4^+FOXP3^+$T cells ($CD3^+$Tregs), and the differential expression was more pronounced in the stromal compartment. TMB-intermediate tumors are mostly grouped with TMB-low cases (Fig. 2, Suppl. Fig. S3, Suppl. Table 3). In order to understand which immune cells had the greatest discriminatory power between TMB-high and the other two categories, we used AUC analysis. Using a combination of seven immune cell types, including $CD208^+$DCs, $CD4^+$T cells, $CD3^+CD4^+$T helper cells, $CD3^+$T cells, $CD3^+CD8^+$, and $CD8^+$cytotoxic T cells, as well as $CD3^+CD8^+FOXP3^+$T cells ($CD8^+$Tregs), combined AUC was 0.99 (Suppl. Fig. S4). Proximity histograms revealed that cytotoxic T cells were significantly closer to tumor cells and T helper cells significantly closer to DCs in TMB-high tumors (Suppl. Fig. S5, Suppl. Table 4) compared with the other two TMB categories.

Intratumoral heterogeneity was pronounced among all PDACs, however, less prominent in TMB-high cases, where immune cells were more evenly distributed among the different tumor areas and more prominent in TMB-intermediate tumors.

3.4. TMB and PD-L1 expression patterns

PD-L1 expression on tumor and/or immune cells was observed in 33.3% (4/12) of TMB-high, 46.4% (13/28) of TMB-intermediate, and 24.8% (30/121) of TMB-low PDACs (overall 47/161; 29.2%; Suppl. Fig. S6). Based on our previous observations, we recognized four distinct PD-L1 patterns comprising two adaptive ("adaptive 1" and "adaptive 2") and two innate type reactions ("constitutive" and "combined") [25]. Adaptive 2 was the predominant pattern in all except TMB-high tumors, in

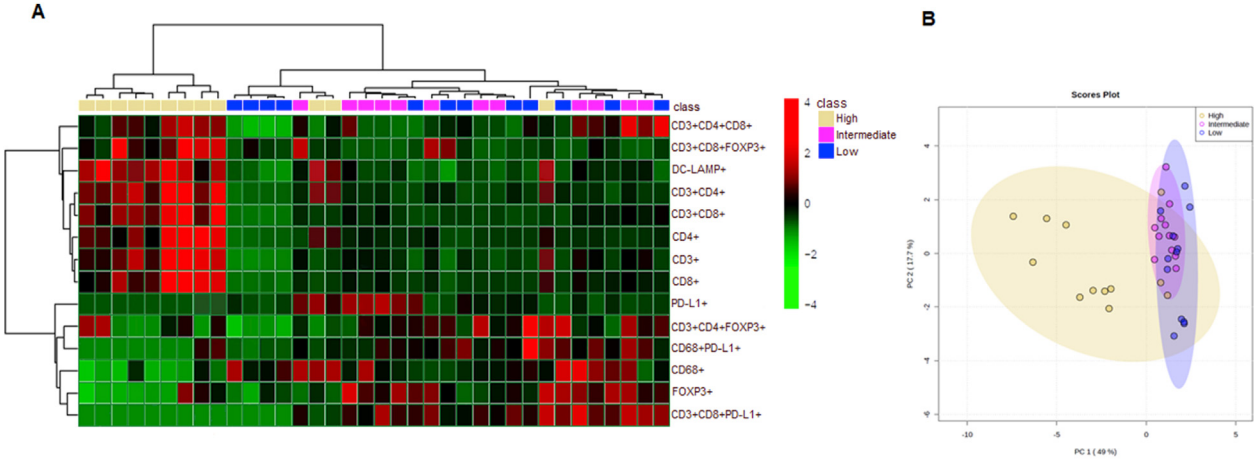

Fig. 3. **A:** Heatmap of the stromal immune cell densities (per mm^2) showing the differential expression of the immune cell populations across the different TMB categories. **B:** Principal component analysis (PCA) performed using stromal immune cell densities shows distinct clustering of TMB-high cases in comparison with TMB-intermediate and TMB-low tumors, which cluster together. Each symbol denotes a patient and 95% confidence ellipses are drawn. The percent variation is explained by first principal component (PC1, x-axis) and the second principal component −2 (PC2, y-axis).

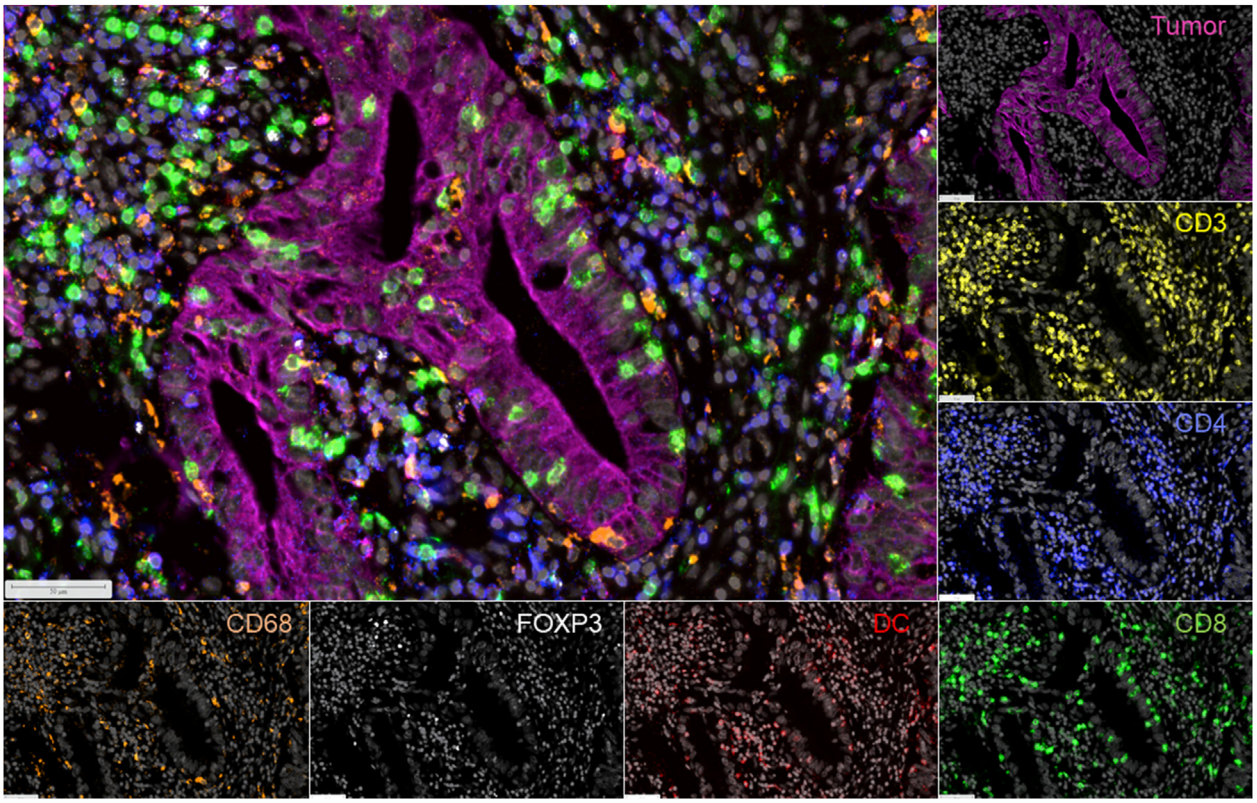

Fig. 4. Image depicting the tumor microenvironment of a microsatellite stable PDAC belonging to the TMB-high category. There are numerous $CD3^+$ T cells (CD3, yellow, in side picture), most of them belonging to the $CD3^+CD4^+$ T helper cell category (CD4, blue). $CD3^+CD8^+$ cytotoxic T cells (CD8, green) are also numerous, and the majority of them are situated in close distance to the tumor cells (Pancytokeratin$^+$, magenta). $CD208^+$ dendritic cells (DC) are depicted in red, $CD3^+CD4^+FOXP3^+$ Tregs (FOXP3) in white, and $CD68^+$TAMs in orange. Nuclear counterstain (DAPI) is grey. Multiplex immunofluorescence (mIF) x200. (For interpretation of the references to color in this figure legend, the reader is referred to the Web version of this article.)

which adaptive 1 pattern was more prominent [20]. No significant correlation between PD-L1 expression and TMB levels or TMB category was observed.

3.5. TMB and microsatellite instability

All five MSI-high cases displayed especially high TMB levels (median: 21.92, mean: 54.05, range 11.46–129), compatible with their hypermutated state.

3.6. TMB and genetic alterations

Sequencing analysis revealed a significant association between TMB categories and mutations in AT-rich interactive domain 1 A (*ARID1A*), a component of the SWitch/Sucrose NonFermentable (SWI/SNF) chromatin remodeling complexes. *ARID1A* mutations were present in 14 PDACs (8.4%) and were more frequent among TMB-high tumors. TMB-high cases represented 21.4% (3/14) of the *ARID1A*-mutated (*ARID1A*mut) and only 6% (9/152) of the *ARID1A*-wild type (*ARID1A*wt) PDACs (p = 123e-23; Suppl. Fig. S7).

The same was true for *ERBB4* mutations (overall 6/166, 3.6%). Three of the six *ERBB4*mut tumors (50%) belonged to the TMB-high category, while only 5.6% (9/160) of the *ERBB4*wt cases were TMB-high (p = 0.033, Suppl. Fig. S7). TMB-high cases were more frequent among *KRAS*wt (29% in *KRAS*wt versus 7% in *KRAS*mut, p = 22e-24) and *SMAD4*wt cases (11% in *SMAD4*wt versus 2% in *SMAD4*mut, p = 3.15e-11). No significant difference was found concerning *TP53, CDKN2A*, or any other mutations across the TMB categories.

3.7. Prognostic significance of TMB

Considering all cases, TMB levels could stratify patients into survival groups, with TMB-high tumors having the best and TMB-low the worst OS and PFS, whereas TMB-intermediate tumors stratified in-between (Fig. 5) in the univariate analysis. We repeated the analysis after removing all LTSs. The remaining 120 conventional PDACs were divided into TMB-low (≤5 mut/Mb, n = 99) and TMB-high + intermediate (>5 mut/Mb, n = 21, including two TMB-high and 19 TMB-intermediate cases). No difference was observed concerning OS or PFS among these groups (Suppl. Fig. S8). Multivariate analysis including various important

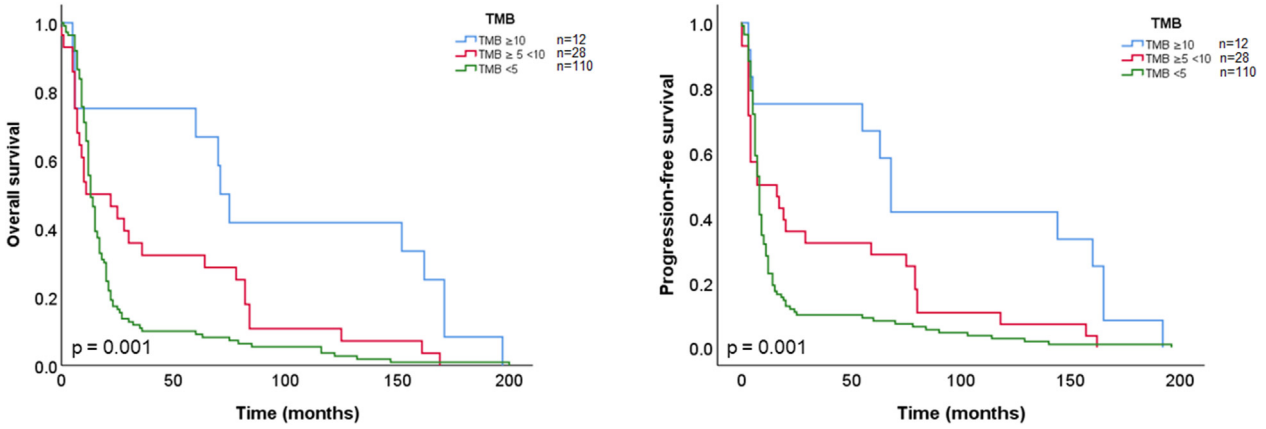

Fig. 5. **A:** Kaplan–Meier curves comparing the overall survival (OS) of PDAC cases with TMB-high (light blue), TMB-intermediate (red), and TMB-low (green) PDACs. **B:** Kaplan–Meier curves comparing the progression-free survival of PDAC cases with TMB-high (light blue), TMB-intermediate (red), and TMB-low (green) PDACs. Statistical comparisons were performed using the log-rank test. (For interpretation of the references to color in this figure legend, the reader is referred to the Web version of this article.)

clinicopathological parameters revealed that only the UICC stage was an independent factor for OS and PFS (Suppl. Tables 5 and 6).

4. Discussion

Here, we show that in surgically resected PDACs (UICC Stage I-III), different TMB levels are associated with distinct immune response patterns in the PDAC TME, as well as different degrees of activation of immune pathways.

TMB-high tumors were particularly enriched in the "immune activated" cluster displaying two- to three-fold upregulation of immune pathway genes, whereas a smaller number clustered into the "immune neutral" cluster. Nevertheless, all TMB-high tumors displayed "hot" TMEs with significantly increased TIL counts, suggesting that the immune response is not purely dependent on the activation of immune pathways and probably related to other factors as well, such as mutation-specific neo-antigens, which represent ideal targets for immunotherapy [26]. Moreover, TMB-high tumors revealed distinct immunoarchitectural patterns, differing strongly from all other PDACs. Although their TME displayed numerous cytotoxic T cells, known to enhance clinical responses following immune checkpoint inhibitors [13,27], TMB-high cases were additionally, particularly rich in T helper cells and DCs. Furthermore, T helper cells were significantly closer to DCs, whereas cytotoxic T cells were closer to tumor cells in TMB-high tumors as compared with all other PDACs, revealing distinct spatio-temporal interactions between T helper cells and DCs and supporting strategic and qualitative differences in the host immune response. Evidence suggests that $CD4^+$T cells can either strengthen or impede $CD8^+$T cell responses by conditioning tumor-infiltrating DCs [28]. Effective anti-tumor responses require a subset of DCs, which produce IL-12 upon sensing interferon γ (IFN-γ) released from neighboring T cells and thus stimulate anti-tumor immunity [29]. Additionally, recent studies have unveiled dynamic interactions between DCs and $CD4^+$T cells in order to prime cytotoxic T cells and direct them against specific antigens [30]. Our findings regarding the immune landscape of TMB-high PDACs support these observations. Moreover, in keeping with the above, both *IFN-γ* and *IL*12 genes were at least two-fold upregulated in TMB-high tumors. Collectively, all this suggests that TMB-high PDACs augmenting neo-antigen-specific $CD4^+$T cells via checkpoint blockade could set in motion dynamic spatio-temporal immune cell interactions leading to robust cytotoxic T cell responses. This might be useful for designing future clinical trials and provides supportive grounds for the introduction of (neo-)adjuvant immunotherapy for TMB-high PDAC patients.

Remarkably, $CD8^+$Tregs ($CD3^+CD8^+FOXP3^+$T cells), shown to control memory responses more efficiently than $CD4^+$Tregs [31], were more numerous in TMB-high PDACs as compared with all other cases, further underscoring the distinct TME profile of TMB-high tumors.

Interestingly, a considerable subset of TMB-intermediate PDACs also displayed an upregulation of immune pathway genes, however, this was not accompanied by significantly elevated TIL counts in their TME, which especially failed to show a significant increase in T helper cells and DCs. This further emphasizes the importance of the quantity and/or quality of neo-antigens in eliciting specific immune responses. Patients with TMB-intermediate PDACs might, however, benefit from novel therapies, such as CD133 mRNA-transferred DCs, as shown in triple-negative breast cancer [32] and vaccine with immunogenic MHC class II peptides, which can elicit specific $CD4^+$T helper anti-tumor responses [33]. Combined with checkpoint blockade, this might lead to measurable clinical efficacy in PDAC patients with TMB-intermediate tumors. In contrast, most TMB-

low PDACs showed an immunosuppressive TME with low TIL and DC counts, accompanied by high counts of TAMs and $CD4^+$Tregs as well as inactivation of immune pathways, rendering these therapies, including immunotherapy, unsuitable for the majority of these patients.

In the present study, all MSI-high cases were also TMB-high. MSI-high tumors are known to be hypermutated, leading to very high TMB levels and the generation of numerous mutation-associated neo-antigens [7,34]. Recent data revealed increased and durable responses to checkpoint blockade in MSI-high/TMB-high tumors [2,3,35]. However, although the prevalence of MSI-high and TMB-high in conventional PDAC is very similar (both <2%), they do not identify the same cases. Indeed, both conventional TMB-high PDACs in our study were MSS, while only about 30% of the TMB-high tumors were also MSI-high. MSS/TMB-high tumors have been identified in several cancer subtypes, including GI cancers [36]. In a recent study, MSS/TMB-high cancers of different histological types displayed longer median PFS after treatment with checkpoint inhibitors [1,37]. These findings suggest that beside dMMR, also other mechanisms may lead to hypermutation and high neo-antigen load. These mechanisms may include alterations in genes such as *ARID1A,* a component of SWitch/Sucrose NonFermentable (SWI/SNF) chromatin remodeling complexes involved in transcriptional activation and repression of select genes. Recent studies have shown that MSS tumors with *ARID1A* mutation may be more susceptible to immune therapy-based treatments and should be recognized as a unique molecular subgroup in immunotherapy trials [38]. Moreover, alterations in *ARID1A* were shown to improve outcomes of advanced pancreatic cancer after immunotherapy [39]. Interestingly, we found a significantly increased prevalence of *ARID1A* mutations in TMB-high tumors as compared with all other PDACs. Although some of these alterations could be attributed to confounding, it seems that the high mutation-specific neo-antigenic load, which is associated with high response rates to immunotherapy, can be achieved through different mechanisms in MSI and MSS PDACs with high TMB levels. This suggests that TMB might expand the pool of PDAC patients that could profit from checkpoint inhibitors. Moreover, in our study, MSS/TMB-high characterized a subset of PDACs that was not only larger than the MSI-high/TMB-high but also different from the PD-$L1^+$subset [25]. This is in accordance with previous studies [40] and further supports that TMB can broaden the population of PDAC patients who could respond to checkpoint blockade. The optimal cutoff between TMB-low and high remains, however, to be defined. It is currently unknown whether individual cutoffs for specific tumor types or a universal cutoff (such as 10 mut/Mb) for all tumors should be adopted [7]. Nevertheless, our findings suggest that in PDAC, a cutoff of 10 mut/Mb detects a subset of patients with the highest probability to respond to checkpoint inhibitors.

TMB can be assessed using whole-exome sequencing (WES) or targeted panel sequencing. Although WES is the "gold standard" for measuring TMB, it is currently not feasible in clinical practice due to its high cost and long turnaround times [7]. In this study, a targeted gene panel covering 1.65 Mb was used, which is well within the range of the internationally recommended panels, including the "Friends of Cancer Research TMB Harmonization Project" [41].

This study has some limitations, including its retrospective nature, as well as the inclusion of patients from only one center and from different PDAC-cohorts. The results require validation from independent data sets.

5. Conclusions

Our results suggest that PDACs of different TMB categories display qualitative differences in their immune responses, which are partly linked to the activation of immune pathways and genetic changes of the tumor cells. PDACs with high TMB levels display strong antitumor immunity, mediated by a T helper cell/DC orchestrated priming of the cytotoxic T cells, independently of their microsatellite state and PD-L1 expression, suggesting that also patients with local/locally advanced MSS TMB-high PDACs might benefit from checkpoint inhibitor therapy.

Financial support

This work was supported in part by the Foundation for Clinical-Experimental Tumor-Research (to E. Karamitopoulou) and Insular Foundation (to B. Gloor). The funders had no involvement in the study design; in the collection, analysis, and interpretation of the data; in the writing of the report; and in the decision to submit the paper for publication.

Author's contributions

Conception and design: E. Karamitopoulou, B. Gloor, A. Perren. **Development of methodology:** E. Karamitopoulou. **Acquisition of data:** A. Andreou, B. Gloor, A. S. Wenning. **Analysis and interpretation of data:** E. Karamitopoulou, A. Andreou, B. Gloor, A. S. Wenning, A. Perren. **Writing, review, and/or revision of the manuscript:** E. Karamitopoulou, A. Andreou, A.S. Wenning, B. Gloor, A. Perren. **Administrative, technical, or material support:** B. Gloor, A. Andreou. **Study supervision:** E. Karamitopoulou, B. Gloor, A. Perren.

Data availability statement

All data are available upon reasonable request. No public databases were used for this study.

Conflict of interest statement

All authors of this manuscript declare no conflict of interest.

Acknowledgements

The authors wish to thank Animesh Acharjee for expert statistical support and the team of the Translational Research Unit (TRU) of the Institute of Pathology, University of Bern for excellent technical assistance.

Appendix A. Supplementary data

Supplementary data to this article can be found online at https://doi.org/10.1016/j.ejca.2022.03.033.

References

[1] Goodman AM, Sokol ES, Frampton GM, Lippman SM, Kurzrock R. Microsatellite-stable tumors with high mutational burden benefit from immunotherapy. Cancer Immunol Res 2019; 7(10):1570–3. https://doi.org/10.1158/2326-6066.CIR-19-0149. PMCID: PMC6774837, 31405947.

[2] Le DT, Uram JN, Wang H, Bartlett BR, Kemberling H, Eyring AD, et al. PD-1 blockade in tumors with mismatch-repair deficiency. N Engl J Med 2015;372(26):2509–20. https://doi.org/10.1056/NEJMoa1500596. PMCID: PMC4481136, 26028255.

[3] Le DT, Durham JN, Smith KN, Wang H, Bartlett BR, Aulakh LK, et al. Mismatch repair deficiency predicts response of solid tumors to PD-1 blockade. Science 2017;357(6349):409–13. https://doi.org/10.1126/science.aan6733. 28596308.

[4] Goodman AM, Kato S, Bazhenova L, Patel SP, Frampton GM, Miller V, et al. Tumor mutational burden as an independent predictor of response to immunotherapy in diverse cancers. Mol Cancer Therapeut 2017;16(11):2598–608. https://doi.org/10.1158/1535-7163.MCT-17-0386. PMCID: PMC5670009, 28835386.

[5] Yarchoan M, Hopkins A, Jaffee EM. Tumor mutational burden and response rate to PD-1 inhibition. N Engl J Med 2017;377(25): 2500–1. https://doi.org/10.1056/NEJMc1713444. 29262275.

[6] Rizvi NA, Hellmann MD, Snyder A, Kvistborg P, Makarov V, Havel JJ, et al. Cancer immunology. Mutational landscape determines sensitivity to PD-1 blockade in non-small cell lung cancer. Science 2015;348(6230):124–8. https://doi.org/10.1126/science.aaa1348. PMCID: PMC4993154, 25765070.

[7] Sha D, Jin Z, Budczies J, Kluck K, Stenzinger A, Sinicrope FA. Tumor mutational burden as a predictive biomarker in solid tumors. Cancer Discov 2020;10(12):1808–25. https://doi.org/10.1126/science.aaa1348. PMCID: PMC7710563, 33139244.

[8] Tran E, Ahmadzadeh M, Lu YC, Gros A, Turcotte S, Robbins PF, et al. Immunogenicity of somatic mutations in human gastrointestinal cancers. Science 2015;350(6266):1387–90. https://doi.org/10.1126/science.aad1253. PMCID: PMC7445892, 26516200.

[9] Desrichard A, Snyder A, Chan TA. Cancer neoantigens and applications for immunotherapy. Clin Cancer Res 2016;22(4):807–12. https://doi.org/10.1158/1078-0432.CCR-14-3175. 26515495.

[10] Yarchoan M, Johnson 3rd BA, Lutz ER, Laheru DA, Jaffee EM. Targeting neoantigens to augment antitumour immunity. Nat Rev Cancer 2017;17(4):209–22. https://doi.org/10.1038/nrc.2016.154. Epub 2017 Feb 24, 28233802.

[11] Subbiah V, Solit DB, Chan TA, Kurzrock R. The FDA approval of pembrolizumab for adult and pediatric patients with tumor mutational burden (TMB) ≥10: a decision centered on empowering patients and their physicians. Ann Oncol 2020;31(9): 1115–8. https://doi.org/10.1038/nrc.2016.154. 32771306.

[12] Gajiwala S, Torgeson A, Garrido-Laguna I, Kinsey C, Lloyd S. Combination immunotherapy and radiation therapy strategies for pancreatic cancer—targeting multiple steps in the cancer immunity cycle. J Gastrointest Oncol 2018;9(6):1014–26. https://doi.org/10.21037/jgo.2018.05.16. PMCID: PMC6286952, 30603120.

[13] Balachandran VP, Łuksza M, Zhao JN, Makarov V, Moral JA, Remark R, et al. Identification of unique neoantigen qualities in long-term survivors of pancreatic cancer. Nature 2017;551(7681):512–6. https://doi.org/10.1038/nature24462. PMCID: PMC6145146, 29132146.

[14] Balachandran VP, Beatty GL, Dougan SK. Broadening the impact of immunotherapy to pancreatic cancer: challenges and opportunities. Gastroenterology 2019;156:2056–72. https://doi.org/10.1053/j.gastro.2018.12.038. PMCID: PMC6486864, 30660727.

[15] Karamitopoulou E. Tumour microenvironment of pancreatic cancer: immune landscape is dictated by molecular and histopathological features. Br J Cancer 2019;121(1):5–14. https://doi.org/10.1038/s41416-019-0479-5. 31110329.

[16] Carstens JL, Correa de Sampaio P, Yang D, Barua S, Wang H, Rao A, et al. Spatial computation of intratumoral T cells correlates with survival of patients with pancreatic cancer. Nat Commun 2017;8:15095. https://doi.org/10.1038/ncomms15095. PMCID: PMC5414182, 28447602.

[17] Vonderheide RH. The immune revolution: a case for priming, not checkpoint. Cancer Cell 2018;33:563–9. https://doi.org/10.1016/j.ccell.2018.03.008. 29634944.

[18] Wartenberg M, Cibin S, Zlobec I, Vassella E, Eppenberger-Castori S, Terracciano L, et al. Integrated genomic and immunophenotypic classification of pancreatic cancer reveals three distinct subtypes with prognostic/predictive significance. Clin Cancer Res 2018;24(18):4444–54. https://doi.org/10.1158/1078-0432.CCR-17-3401. 29661773.

[19] Torphy RJ, Zhu Y, Schulick RD. Immunotherapy for pancreatic cancer: barriers and breakthroughs. Ann Gastroenterol Surg 2018;2(4):274–81. https://doi.org/10.1002/ags3.12176. PMCID: PMC6036358, 30003190.

[20] Katsuta E, Huyser M, Yan L, Takabe K. A prognostic score based on long-term survivor unique transcriptomic signatures predicts patient survival in pancreatic ductal adenocarcinoma. Am J Cancer Res 2021 Sep 15;11(9):4294–307. PMCID: PMC8493373, 34659888.

[21] Belfiori G, Crippa S, Francesca A, Pagnanelli M, Tamburrino D, Gasparini G, et al. Long-term survivors after upfront resection for pancreatic ductal adenocarcinoma: an actual 5-year analysis of disease-specific and post-recurrence survival. Ann Surg Oncol 2021 Dec;28(13):8249–60. https://doi.org/10.1245/s10434-021-10401-7. 34258720.

[22] Wang H, Liu B, Wei J. Beta2-microglobulin (B2M) in cancer immunotherapies: biological function, resistance and remedy. Cancer Lett 2021 Oct 1;517:96–104. https://doi.org/10.1016/j.canlet.2021.06.008. 34129878.

[23] Leon F, Seshacharyulu P, Nimmakayala RK, Chugh S, Karmakar S, Nallasamy P, et al. Reduction in O-glycome induces differentially glycosylated CD44 to promote stemness and metastasis in pancreatic cancer. Oncogene 2022 Jan;41(1):57–71. https://doi.org/10.1038/s41388-021-02047-2. PMCID: PMC8727507, 34675409.

[24] Navas T, Kinders RJ, Lawrence SM, Ferry-Galow KV, Borgel S, Hollingshead MG, et al. Clinical evolution of epithelial-mesenchymal transition in human carcinomas. Cancer Res 2020 Jan 15;80(2):304–18. https://doi.org/10.1158/0008-5472.CAN-18-3539. PMCID: PMC8170833 doi: 31732654.

[25] Karamitopoulou E, Andreou A, Pahud de Mortanges A, Tinguely M, Gloor B, Perren A. PD-1/PD-L1-Associated immunoarchitectural patterns stratify pancreatic cancer patients into

prognostic/predictive subgroups. Cancer Immunol Res 2021; 9(12):1439–50. https://doi.org/10.1158/2326-6066.CIR-21-0144. 34526323.

[26] Brightman SE, Naradikian MS, Miller AM, Schoenberger SP. Harnessing neoantigen specific CD4 T cells for cancer immunotherapy. J Leukoc Biol 2020;107(4):625–33. https://doi.org/10.1002/JLB.5RI0220-603RR. PMCID: PMC7793607, 32170883.

[27] Cristescu R, Mogg R, Ayers M, Murphy E, Yearley J, Sher X, et al. Pan-tumor genomic biomarkers for PD-1 checkpoint blockade-based immunotherapy. Science 2018;362(6411):eaar3593. https://doi.org/10.1126/science.aar3593. Erratum in: Science. 2019 Mar 1; 363(6430). PMID: 30819935 DOI: 10.1126/science.aax1384, 30309915.

[28] Allan RS, Waithman J, Bedoui S, Jones CM, Villadangos JA, Zhan Y, et al. Migratory dendritic cells transfer antigen to a lymph node-resident dendritic cell population for efficient CTL priming. Immunity 2006;25(1):153–62. https://doi.org/10.1016/j.immuni.2006.04.017. 16860764.

[29] Garris CS, Arlauckas SP, Kohler RH, Trefny MP, Garren S, Piot C, et al. Successful anti-PD-1 cancer immunotherapy requires T cell-dendritic cell crosstalk involving the cytokines IFN-γ and IL-12. Immunity 2018;49(6):1148–61. https://doi.org/10.1016/j.immuni.2018.09.024. PMCID: PMC6301092, 30552023.

[30] Hor JL, Whitney PG, Zaid A, Brooks AG, Heath WR, Mueller SN. Spatiotemporally distinct interactions with dendritic cell subsets facilitates CD4+ and CD8+ T cell activation to localized viral infection. Immunity 2015;43(3):554–65. https://doi.org/10.1016/j.immuni.2015.07.020. 26297566.

[31] Flippe L, Bézie S, Anegon I, Guillonneau C. Future prospects for CD8+regulatory T cells in immune tolerance. Immunol Rev 2019;292: 209–24. https://doi.org/10.1111/imr.12812. PMCID: PMC7027528, 31593314.

[32] Tay ASS, Amano T, Edwards LA, Yu JS. CD133 mRNA-transfected dendritic cells induce coordinated cytotoxic and helper T cell responses against breast cancer stem cells. Mol Ther Oncolytics 2021; 22:64–71. https://doi.org/10.1016/j.omto.2021.05.006. PMCID: PMC8403713, 34485687.

[33] Basu A, Albert GK, Awshah S, Datta J, Kodumudi KN, Gallen C, et al. Identification of immunogenic MHC class II human HER3 peptides that mediate anti-HER3 CD4+ Th1 responses and potential use as a cancer vaccine. Cancer Immunol Res 2022;10(1): 108–25. https://doi.org/10.1158/2326-6066.CIR-21-0454. 34785506.

[34] Campbell BB, Light N, Fabrizio D, Zatzman M, Fuligni F, de Borja R, et al. Comprehensive analysis of hypermutation in human cancer. Cell 2017;171(5):1042–56. https://doi.org/10.1016/j.cell.2017.09.048. PMCID: PMC5849393, 29056344.

[35] Germano G, Lamba S, Rospo G, Barault L, Magrì A, Maione F, et al. Inactivation of DNA repair triggers neoantigen generation and impairs tumour growth. Nature 2017;552(7683):116–20. https://doi.org/10.1038/nature24673. 29186113.

[36] Salem ME, Puccini A, Grothey A, Raghavan D, Goldberg RM, Xiu J, et al. Landscape of tumor mutation load, mismatch repair deficiency, and PD-L1 expression in a large patient cohort of gastrointestinal cancers. Mol Cancer Res 2018;16(5):805–12. https://doi.org/10.1158/1541-7786.MCR-17-0735. PMCID: PMC6833953, 29523759.

[37] Valero C, Lee M, Hoen D, Zehir A, Berger MF, Seshan VE, et al. Response rates to anti-PD-1 immunotherapy in microsatellite-stable solid tumors with 10 or more mutations per megabase. JAMA Oncol 2021;7(5):739–43. https://doi.org/10.1001/jamaoncol.2020.7684. 33599686.

[38] Mehrvarz Sarshekeh A, Alshenaifi J, Roszik J, Manyam GC, Advani SM, Katkhuda R, et al. ARID1A mutation may define an immunologically active subgroup in patients with microsatellite stable colorectal cancer. Clin Cancer Res 2021;27(6):1663–70. https://doi.org/10.1158/1078-0432.CCR-20-2404. PMCID: PMC7956157, 33414133.

[39] Botta GP, Kato S, Patel H, Fanta P, Lee S, Okamura R, Kurzrock R. SWI/SNF complex alterations as a biomarker of immunotherapy efficacy in pancreatic cancer. JCI Insight 2021 Sep 22;6(18):e150453. https://doi.org/10.1172/jci.insight.150453. PMCID: PMC8492298 doi: 34375311.

[40] Yarchoan M, Albacker LA, Hopkins AC, Montesion M, Murugesan K, Vithayathil TT, et al. PD-L1 expression and tumor mutational burden are independent biomarkers in most cancers. JCI Insight 2019;4(6):e126908. https://doi.org/10.1172/jci.insight.126908. PMCID: PMC6482991, 30895946.

[41] Vega DM, Yee LM, McShane LM, Williams PM, Chen L, Vilimas T, et al., TMB Consortium. Aligning tumor mutational burden (TMB) quantification across diagnostic platforms: phase II of the Friends of Cancer Research TMB Harmonization Project. Ann Oncol 2021;32(12):1626–36. https://doi.org/10.1016/j.annonc.2021.09.016. 34606929.